Alternative haplotypes of antigen processing genes in zebrafish diverged early in vertebrate evolution

Sean C. McConnell[a,1], Kyle M. Hernandez[b], Dustin J. Wcisel[c,d], Ross N. Kettleborough[e], Derek L. Stemple[e], Jeffrey A. Yoder[c,d,f], Jorge Andrade[b], and Jill L. O. de Jong[a,1]

[a]Section of Hematology-Oncology and Stem Cell Transplant, Department of Pediatrics, The University of Chicago, Chicago, IL 60637; [b]Center for Research Informatics, The University of Chicago, Chicago, IL 60637; [c]Department of Molecular Biomedical Sciences, College of Veterinary Medicine, North Carolina State University, Raleigh, NC 27607; [d]Genomic Sciences Graduate Program, North Carolina State University, Raleigh, NC 27607; [e]Vertebrate Development and Genetics, Wellcome Trust Sanger Institute, Cambridge CB10 1SA, United Kingdom; and [f]Comparative Medicine Institute, North Carolina State University, Raleigh, NC 27607

Edited by Peter Parham, Stanford University School of Medicine, Stanford, CA, and accepted by Editorial Board Member Peter Cresswell June 23, 2016 (received for review May 16, 2016)

Antigen processing and presentation genes found within the MHC are among the most highly polymorphic genes of vertebrate genomes, providing populations with diverse immune responses to a wide array of pathogens. Here, we describe transcriptome, exome, and whole-genome sequencing of clonal zebrafish, uncovering the most extensive diversity within the antigen processing and presentation genes of any species yet examined. Our CG2 clonal zebrafish assembly provides genomic context within a remarkably divergent haplotype of the core MHC region on chromosome 19 for six expressed genes not found in the zebrafish reference genome: *mhc1uga*, proteasome-β 9b (*psmb9b*), *psmb8f*, and previously unknown genes *psmb13b*, *tap2d*, and *tap2e*. We identify ancient lineages for Psmb13 within a proteasome branch previously thought to be monomorphic and provide evidence of substantial lineage diversity within each of three major trifurcations of catalytic-type proteasome subunits in vertebrates: Psmb5/Psmb8/Psmb11, Psmb6/Psmb9/Psmb12, and Psmb7/Psmb10/Psmb13. Strikingly, nearby *tap2* and *MHC class I* genes also retain ancient sequence lineages, indicating that alternative lineages may have been preserved throughout the entire MHC pathway since early diversification of the adaptive immune system ∼500 Mya. Furthermore, polymorphisms within the three MHC pathway steps (antigen cleavage, transport, and presentation) are each predicted to alter peptide specificity. Lastly, comparative analysis shows that antigen processing gene diversity is far more extensive than previously realized (with ancient coelacanth *psmb8* lineages, shark *psmb13*, and *tap2t* and *psmb10* outside the teleost MHC), implying distinct immune functions and conserved roles in shaping MHC pathway evolution throughout vertebrates.

comparative genomics | proteasome and TAP evolution | major histocompatibility | MHC class I pathway | CG2 clonal zebrafish

Genetic diversity promotes robust immune function. MHC gene polymorphism provides a classic example, because human populations carry hundreds of MHC class I alleles (*MHCI*), which present antigens to activate an immune response (1). Variation observed between alleles of immune genes may exceed levels explained by simple accumulation of mutations within a species over time. For example, sequence variation within human *MHC* genes has been traced back 10–50 My (2–4), including allelic variants shared with other primate species. Transspecies polymorphism explains this observation by positing that some alleles survive multiple speciation events, thereby providing descendant species with higher functional sequence diversity (5). Starting with this diversity, balancing selection preserves polymorphism within populations during conditions when no single allele is optimized for all environments, with a disproportionate impact on immune loci (6). Some nonmammalian vertebrates, such as bony fish, frogs, and sharks, maintain MHC polymorphism at even higher levels than mammals (7–10), implying preservation of ancient alleles across different species.

Recent genomic studies have offered considerable insights into the evolution of the vertebrate adaptive immune system by comparing phylogenetically divergent species (11–14). Throughout vertebrates, gene linkage within the MHC region is highly conserved. For example, *MHCI* and antigen processing genes remain tightly linked in sharks, members of the oldest vertebrate lineage to maintain an MHC-mediated adaptive immune system (15, 16). This tight linkage is also highly conserved in bony fish (17–19) as well as in additional nonmammalian jawed vertebrates, such as frogs (20). Coevolution of *MHCI* and antigen processing genes is facilitated by their close physical proximity in the genome, leading to coinheritance of alleles throughout the MHC pathway with compatible peptide specificities. Juxtaposition of these genes into compact haplotypes may, thus, provide a foundation for

Significance

Antigen presentation genes are exceptionally polymorphic, enhancing immune defense. Polymorphism within additional components of the MHC pathway, particularly the antigen processing genes, may also shape immune responses. Using transcriptome, exome, and whole-genome sequencing to examine immune gene variation in zebrafish, we uncovered several antigen processing genes not found in the reference genome clustered within a deeply divergent haplotype of the core MHC locus. Our data provide evidence that these previously undescribed antigen processing genes retain ancient alternative sequence lineages, likely derived during the formation of the adaptive immune system, and represent the most divergent collection of antigen processing and presentation genes yet identified. These findings offer insights into the evolution of vertebrate adaptive immunity.

Author contributions: S.C.M. and J.L.O.d. designed research; S.C.M. and J.L.O.d. performed research; S.C.M. and J.L.O.d. analyzed data; S.C.M. and J.L.O.d. wrote the paper; K.M.H. and J.A. contributed the de novo genomic assembly; D.J.W. and J.A.Y. contributed transcriptome assembly data; and R.N.K. and D.L.S. contributed whole-exome sequence data.

The authors declare no conflict of interest.

This article is a PNAS Direct Submission. P.P. is a Guest Editor invited by the Editorial Board.

Data deposition: Exome data for CG1 clonal zebrafish have been deposited in the NCBI Sequence Read Archive (SRA; accession nos. ERS216437, ERS216444, ERS216451, and ERS216458), and exome data for CG2 clonal zebrafish have been deposited in the NCBI SRA (accession nos. ERS216465, ERS216472, ERS216479, and ERS216486). The CG2 immune tissue RNA-Seq data (nonnormalized and normalized) have been deposited in the NCBI SRA (accession no. SRP057116). The nonnormalized and normalized CG2 immune tissue transcript assembly data have been deposited in the Transcriptome Shotgun Assembly (TSA; accession nos. GDQH00000000 and GDQQ00000000). Genomic sequencing data from CG2 clonal zebrafish have been deposited in the NCBI SRA (accession no. SRP062426), and the CG2 genomic assembly has been deposited in the NCBI Whole Genome Shotgun database (accession no. LKPD00000000). Transcripts associated with zebrafish core MHC haplotype D are provided in in Dataset S3, predicted amino acid sequences for the CG2 haplotype D antigen processing gene transcripts are provided in Dataset S4, and genomic scaffold sequences identified from haplotype D are provided in Dataset S5.

[1]To whom correspondence may be addressed. Email: scmcconnell@uchicago.edu or jdejong@peds.bsd.uchicago.edu.

This article contains supporting information online at www.pnas.org/lookup/suppl/doi:10.1073/pnas.1607602113/-/DCSupplemental.

www.pnas.org/cgi/doi/10.1073/pnas.1607602113

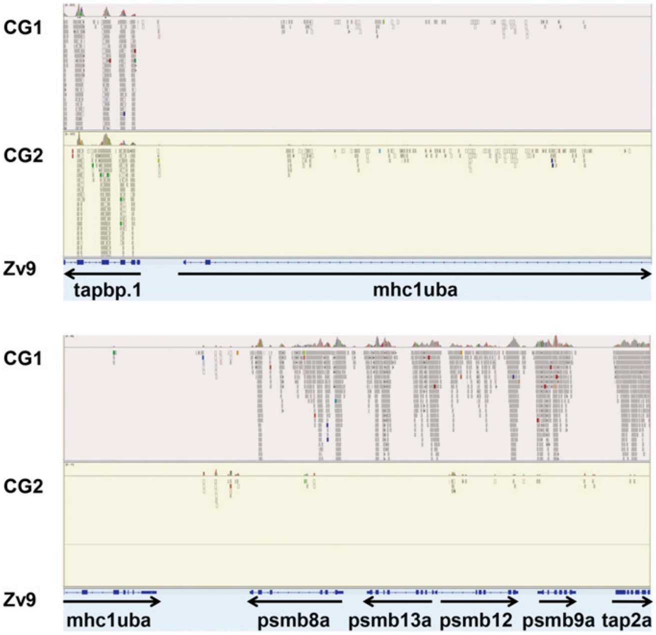

Fig. 1. The core MHC region in clonal zebrafish. Aligned reads are shown for representative exomes from clonal golden zebrafish lines (CG1 and CG2) that map to the core MHC region on chromosome 19 of the Zv9 zebrafish reference genome (coordinates 7689327–7748684). Refseq annotated exons are shown below with transcriptional orientations.

the evolution of MHC pathways functioning with more highly specialized peptide repertoires (21).

In contrast, MHC gene arrangements in mammals generally differ from those of other vertebrates, including much greater distance between the *MHCI* and antigen processing genes. Mammalian antigen processing genes are instead found in the class II region of the MHC, where they are far removed from the *MHCI* genes found in the class I region. This physical distance limits the capacity of these genes to coevolve distinct peptide specificities, because increased recombination is likely to deter the specialization of alleles upstream in the MHC pathway because of the potential for downstream incompatibility. Accordingly, compared with nonmammalian vertebrates, mammalian antigen processing genes are much less polymorphic, and mammalian MHC pathway diversity remains instead focused primarily in the *MHCI* genes. These findings are consistent with an immune strategy favoring the cleavage and transport of a more "generic" peptide repertoire, with greater emphasis on the downstream peptide binding specificities using a collection of diverse *MHCI* molecules (21–23).

Some notable exceptions to these observations have been reported. For example, rat *MHCI* genes are found more tightly linked with antigen processing genes than in other rodents, such as mice, consistent with rat haplotypes having more specialized antigen transport (TAP) alleles exhibiting either "restrictive" or "permissive" peptide repertoires (24). Chickens represent another interesting exception, because antigen processing genes from the first stage of the MHC pathway, the inducible proteasome subunits proteasome-β 8–10 (*psmb8–10*), are altogether missing (25). However, this lack of inducible proteasome subunits in chickens does not seem to have reduced the capacity for polymorphic antigen transport genes, encoding the TAP subunits, to coevolve distinctive peptide specificities with coinherited *MHCI* alleles (26).

In teleosts (bony fish), MHC arrangements are similar to other nonmammalian vertebrates, but important differences are observed. Teleost antigen processing genes are found adjacent to their *MHCI* genes, despite the teleost MHCI and MHCII regions being distinctively unlinked (27). Teleost *MHCI* genes retain ancient lineages, with sequences estimated to be hundreds of millions of years old (9). These lineages are ancient compared with other vertebrates, such as mammals, where *MHCI* lineages appear to be much younger at millions or tens of millions of years old. Furthermore, the antigen processing gene *psmb8* has also been shown to retain ancient sequence lineages in teleosts that are hundreds of millions of years old (28). Finally, an additional set of unique and perhaps teleost-specific proteasome subunit genes was previously linked to teleost *MHCI* genes (17–19, 29), and one of these genes referred to as *psmb10* displayed limited (believed nonfunctional) polymorphism (30). However, few other studies have examined these genes in detail.

We recently characterized classical *MHCI* genes from six divergent haplotypes found in clonal and selectively bred zebrafish (31) and identified remarkable additional haplotype variability. Unlike in most other species examined, we found that distinct zebrafish MHC haplotypes express altogether different sets of *MHCI* genes, which are each linked to the divergent antigen processing gene *psmb8a* or *psmb8f*. Copy number variation for nearby *tap2* and *tapbp* genes also accompanied these other haplotypic differences. Revealing the full extent of additional haplotype diversity would require genomic sequencing; indeed, to date, such sequences have been lacking for haplotypes containing the ancient *psmb8f* lineage. Intriguingly, additional putative antigen processing genes from zebrafish have been found only in expression libraries, despite the availability of a high-quality reference genome (32). Such "orphan" sequences may be associated with alternative haplotypes (for example, the core MHC region on zebrafish chromosome 19), where the genes are likely to maintain central roles in immune function. Incorporating these divergent sequences into genomic assemblies has great potential to further improve our understanding of the formation of the adaptive immune system, an event closely associated with the origin of all vertebrates (33, 34).

Here, we report the genomic sequence for the core MHC region of CG2 clonal zebrafish. Our assembly uncovers genes from an alternative haplotype and places them into genomic context. By examining the sequence properties of these divergent zebrafish antigen processing genes, we provide evidence that they represent ancient lineages, including polymorphic residues likely to contribute to immune function. In addition, our comparative analysis across vertebrates yields a more comprehensive understanding of the relationships and extensive diversity found among these antigen processing and presentation genes, revealing additional genes in species such as zebrafish and coelacanths, and evidence of ancient lineages and haplotypes that have shaped the evolution of the MHC pathway.

Results

Whole-Exome Sequencing of Clonal Zebrafish. To identify potential variants in immune loci, we first performed whole-exome sequencing of two different lines of homozygous diploid, clonal golden zebrafish: CG1 and CG2 (35, 36). Analysis of our exome data revealed distinctive patterns of haplotypic variation. For example, for both clonal zebrafish exomes, essentially no reads were aligned to the *mhc1uba* gene on chromosome 19 of the reference genome (Fig. 1). For the CG2 clonal zebrafish line, this absence of aligned reads was also found for additional genes adjacent to *mhc1uba*. The pattern extended throughout a region of ∼100 kb, encompassing the *MHCI* genes as well as linked antigen processing genes—*psmb8a*, *psmb9a*, *psmb12*, *psmb13a*, and *tap2a*. In contrast, numerous reads from CG1 matched antigen processing exons from the Zv9 reference genome. Therefore, the extended MHC variation seems to be specific for CG2.

Sequencing and de Novo Assembly of a Divergent MHC Locus. To identify divergent sequences potentially missed by the hybridization-based exome sequencing approach, we performed whole-genome sequencing of CG2 clonal zebrafish. Starting with paired end reads obtained at 25× coverage, we generated genomic scaffolds by de novo assembly. Most of our draft CG2 genome assembly matched the reference genome, with 72,406 scaffolds (of 73,507 with size >1 kb) having an average of 95.4% sequence identity. However,

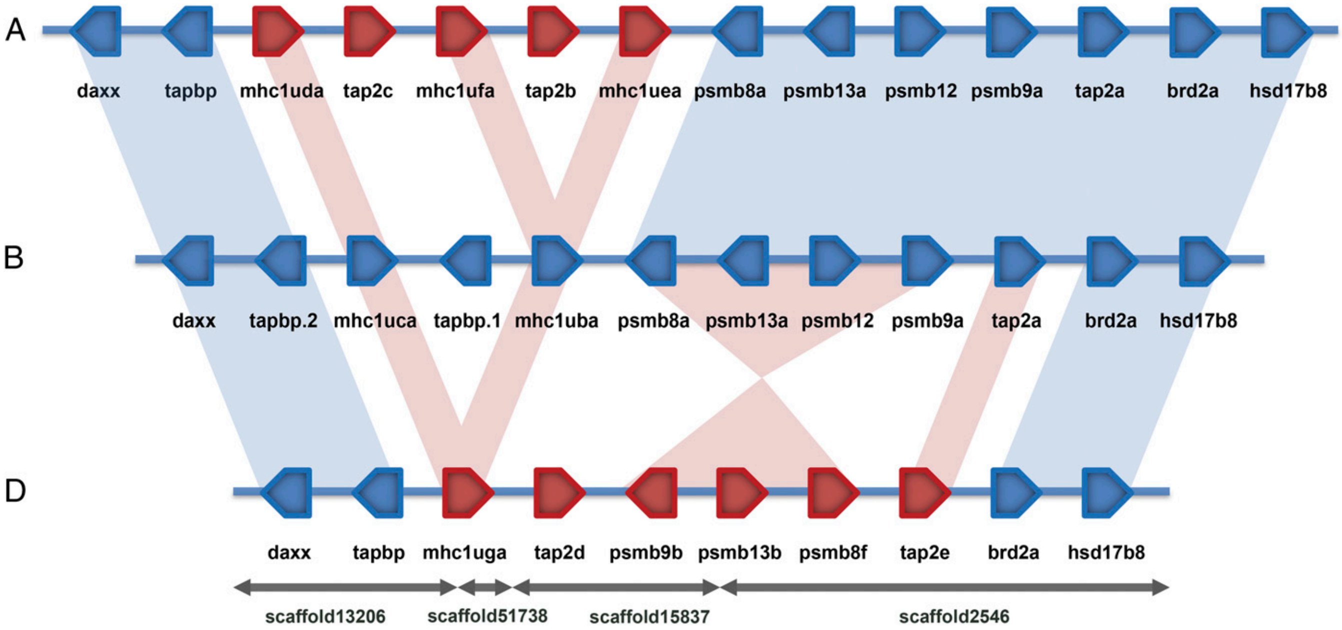

Fig. 2. Comparison of zebrafish core MHC haplotypes. Genes highly conserved with the reference haplotype B are shown in blue, and these highly conserved relationships are illustrated with blue shading. Genes divergent from the reference haplotype B are shown in red, and divergent gene relationships with haplotype B are illustrated with red shading. Haplotype A is part of an alternative haplotypic assembly of sequences derived from AB zebrafish (VEGA59 chromosome AB: 9329627–9629628), haplotype B is from the reference genome derived primarily from Tuebingen zebrafish (Zv9 chromosome 19: 7623109–78026601), and haplotype D was obtained by de novo assembly of genomic sequences from CG2 clonal golden zebrafish (this study).

some scaffolds did not align to the reference genome, indicating candidate regions of the CG2 zebrafish genome harboring extensive haplotypic variation.

We focused on the chromosome 19 core MHC locus, where considerable haplotypic variation was observed previously (17, 31). BLAST searches of our CG2 genomic database identified scaffolds containing MHC flanking genes, including *tapbp* and *brd2a* (Fig. 2). These scaffolds also included *mhc1uga* and *psmb8f* that we previously mapped with linkage and expression data (using offspring of MHC haplotype compound heterozygous fish) to the core MHC haplotype D of CG2 clonal zebrafish (31).

Scaffold orientation was inferred by using predicted gene models, which were improved by RNA sequencing (RNA-Seq) data, and also, the presence of conserved MHC flanking sequences (*SI Appendix*, Table S1). Two of three scaffold junctions occurred within introns, with these two junctions together imparting orientation for four of the scaffolds, whereas the two distal scaffolds were anchored using their conserved MHC flanking sequences. These distal regions from the divergent haplotype D assembly, including the *tapbp*, *daxx*, *brd2a*, and *hsd17b8* genes, were highly conserved with haplotype B found in the reference genome. The conserved flanking regions together with linkage data for *psmb8f* and *mhc1uga* (31) anchor the scaffolds as a divergent MHC haplotype on chromosome 19.

Comparison of Zebrafish Core MHC Haplotypes. Genomic sequences are available for three zebrafish core MHC haplotypes: A from a prior AB assembly, B from the Zv9 reference genome, and D derived from CG2 clonal zebrafish in this study. All three sequenced zebrafish MHC haplotypes are flanked by conserved chromosome 19 sequences (Fig. 2) as illustrated by highlighting conserved genes *daxx* and *tapbp* on the left and *brd2a* and *hsd17b8* on the right. Of eight genes found in between these flanking genes in reference haplotype B, five genes are shared with haplotype A that maintain high levels of sequence identity: *psmb8a*, *psmb13a*, *psmb12*, *psmb9a*, and *tap2a*. In contrast, differences between haplotypes A and B are evident for the divergent MHCI gene sequences. Three MHCI genes are found for haplotype A (*mhc1uda*, *mhc1ufa*, and *mhc1uea*) compared with two genes for haplotype B (*mhc1uca* and *mhc1uba*). Differences are also observed for the duplicated genes found between the MHCI genes, where two genes are present for haplotype A (*tap2c* and *tap2b*) compared with one gene for haplotype B (*tapbp.1*). Nevertheless, these two haplotypes share highly conserved antigen processing genes *psmb8a*, *psmb13a*, *psmb12*, *psmb9a*, and *tap2a*.

In contrast, haplotype D from CG2 zebrafish shares none of eight central genes from haplotype B (Fig. 2). Haplotype D instead carries a single divergent MHCI gene *mhc1uga* and two divergent *tap2* genes *tap2d* and *tap2e* as well as an apparent inversion containing the divergent *psmb9b*, *psmb13b*, and *psmb8f* genes. Although each of three zebrafish core MHC haplotypes maintains distinctive genomic sequence arrangements, haplotype D remains most divergent in sequence, including each of the antigen processing genes.

Genes in a Divergent Zebrafish Core MHC Haplotype. Genomic context for the *psmb8f* and *mhc1uga* genes was markedly different from the corresponding region of the reference genome. Analysis of the divergent haplotype D assembly revealed four additional gene sequences that are not present in the reference zebrafish genome: *tap2d*, *psmb9b*, *psmb13b*, and *tap2e* (Fig. 2). Thus, our assembly incorporates previously unknown or unplaced genes into an alternative haplotype for the core MHC locus on zebrafish chromosome 19.

Each of the genes from haplotype D also had corresponding transcripts identified within the RNA-Seq database derived from CG2 immune tissues (*SI Appendix*, Table S1). These data provide direct experimental evidence of expression for each gene found within the divergent haplotype D genomic assembly, including transcripts for the *tapbp*, *daxx*, *brd2a*, and *hsd17b8* genes as well as the *tap2d*, *psmb9b*, *psmb13b*, *tap2e*, *mhc1uga*, and *psmb8f* genes. Consistent with our alternative haplotype assembly (Fig. 2), no RNA-Seq transcripts were identified from CG2 immune tissues for seven genes associated with the reference core MHC haplotype B: *mhc1uba*, *mhc1uca*, *psmb8a*, *psmb9a*, *psmb12*, *psmb13a*, and *tap2a*.

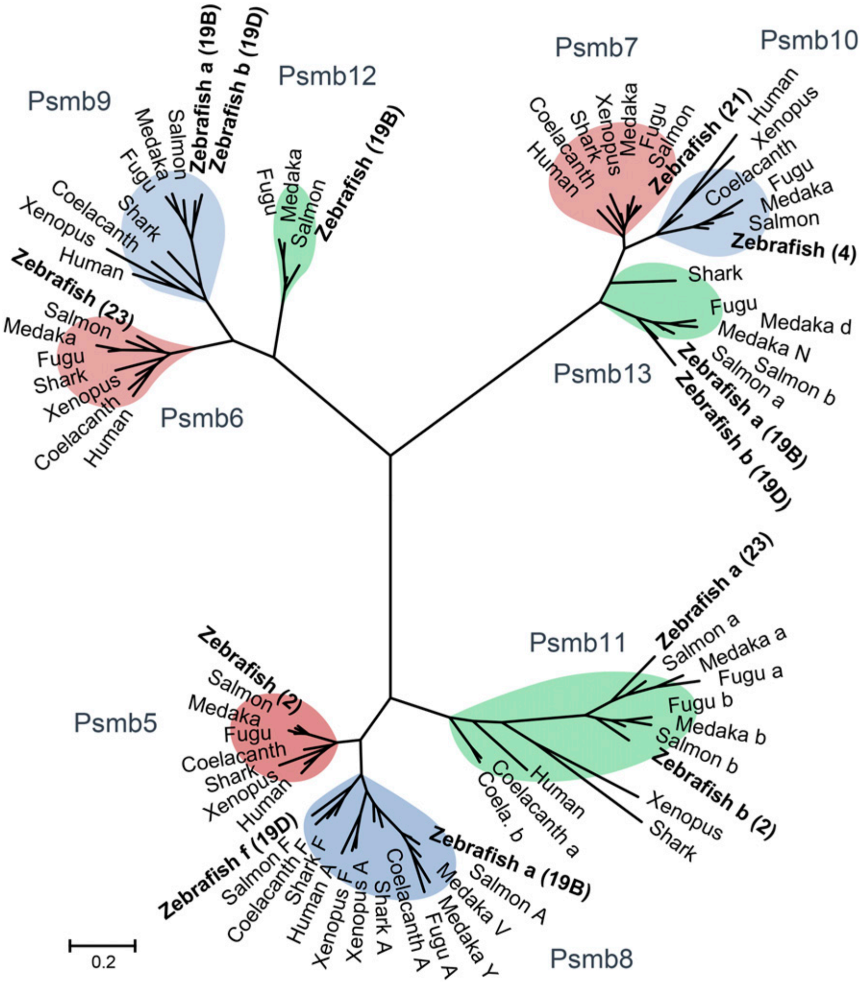

Fig. 3. Phylogenetic relationships for proteasome subunits from zebrafish and additional vertebrates. Multimeric proteasomes have interchangeable catalytic subunits in most jawed vertebrates. Constitutive proteasome, immunoproteasome, and intermediate proteasome forms each degrade intracellular proteins into the peptide fragments that are presented by MHC molecules at the cell surface. The three ancestral PSMB subunits with distinct catalytic activities (Psmb5, Psmb6, and Psmb7) segregate into three major branches in the phylogenetic tree. These three constitutive proteasome subunits Psmb5 (LMPX), Psmb6 (LMPY), and Psmb7 (LMPZ) are replaced by IFN-inducible immunoproteasome subunits Psmb8 (LMP7), Psmb9 (LMP2), and Psmb10 (MECL-1), respectively, during an immune response. In addition, the thymoproteasome subunit Psmb11 replaces Psmb5 and Psmb8 specifically in the thymus. These more specialized, nonconstitutive, proteasome subunits seem to be specific to jawed vertebrates (87). Deduced amino acid sequences were used to construct maximum likelihood trees. For clarity only, the subunit encoded by the Zv9 reference genome is shown for three constitutive proteasome (Psmb5, Psmb6, and Psmb7) and two thymoproteasome (Psmb11a and Psmb11b) subunits. Chromosome locations for zebrafish subunits are provided in parentheses, including haplotype associations when applicable. Additional phylogenetic trees with bootstrap values and other species are provided in *SI Appendix*, Figs. S5–S7. Sequences are provided in Dataset S1.

Phylogenetic Analysis of Zebrafish Proteasome Subunits. All three forms of proteasome subunits (constitutive, immunoproteasome, and thymoproteasome) are conserved in zebrafish (Fig. 3), including single copies found for the three constitutive subunits (Psmb5, Psmb6, and Psmb7). The thymoproteasome subunits Psmb11a and Psmb11b in zebrafish represent teleost-specific gene duplicates associated with an ancient teleost-specific whole-genome duplication (37). Consistent with other largely monomorphic MHC pathway genes that are found outside the core MHC locus, such as *tap1* (*SI Appendix*, Table S2), these three constitutive proteasome and two thymoproteasome subunits, all non-MHC linked, each share 99 to 100% sequence identity between the reference genome and CG2 zebrafish genome assemblies.

In contrast to the constitutive and thymoproteasome subunits that are more conserved, three MHC-linked immunoproteasome subunits (Psmb8, Psmb9, and Psmb13) have divergent lineages in zebrafish (Table 1). These different genes are maintained in a haplotype-specific manner. Phylogenetic relationships, thus, reveal the presence of ancient lineages for each of three major branches of proteasomal subunits comparing the zebrafish Psmb8f, Psmb9b, and Psmb13b sequences encoded by core MHC haplotype D on chromosome 19 with the Psmb8a, Psmb9a, and Psmb13a sequences encoded by haplotype B.

Previous studies have shown how the Psmb8a and Psmb8f lineages maintain ancient evolutionary histories approaching 500 My (28). Other proteasomal subunits also maintain distinct lineages, such as the Psmb9a and Psmb9b subunits from different zebrafish core MHC haplotypes (Fig. 3). In addition, Psmb12 is not found in the core MHC haplotype D or the rest of the CG2 genome, providing evidence for presence/absence variation of this subunit in zebrafish (Figs. 1 and 2).

Sequence Properties for the Zebrafish Psmb13b. Psmb13a and the Psmb13b subunit also maintain ancient lineages. Zebrafish Psmb13b shares levels of divergence with the zebrafish Psmb13a sequence (Fig. 4) that are similar to levels shared with sequences from other teleost species, including salmon (69 to 72% amino acid identity). This divergence pattern, with Psmb13b appearing as the most basal sequence, indicates that Psmb13a and Psmb13b sequences have been independently evolving for ~300 My, since the time of the last common ancestor of zebrafish and salmonids (38). Comparison of the different zebrafish Psmb13 subunits with sequences from other species, thus, provides clear evidence for ancient lineages.

The sequence alignment (Fig. 4) shows that many residues are unique for zebrafish Psmb13b and not found in Psmb13a or sequences identified from other species. However, one potentially important substitution found in Psmb13b is also shared by sequences from additional species. This amino acid substitution at position 53 of the mature proteasomal subunit may influence peptide cleavage specificity (39, 40). At this critical residue, zebrafish Psmb13b has an uncharged glutamine (Q) instead of the charged glutamic acid (E) residue found in most fish species. Notably, sequences from fugu (*Takifugu rubripes*) and damselfish (*Stegastes partitus*) also carry the E53Q substitution, suggesting that this is a functionally important polymorphism.

The E53 residue found in zebrafish Psmb13a is also found in other sequences from this family of subunits, including the human PSMB10 immunoproteasome subunit (*SI Appendix*, Fig. S1). The

Table 1. Comparison of genes from the haplotype 19D assembly with genes from haplotype 19B from the zebrafish reference genome

Haplotype D gene*	Identity, %†	Haplotype B gene‡	Chromosome§
daxx	99	*daxx*	19
tapbp	98	*tapbp*	19
mhc1uga	49	*mhc1uba*	19
tap2d	65	*tap2a*	19
psmb9b	86	*psmb9a*	19
psmb13b	71	*psmb13a*	19
psmb8f	64	*psmb8a*	19
tap2e	50	*tap2a*	19
brd2a	100	*brd2a*	19
hsd17b8	99	*hsd17b8*	19

*Sequences from core MHC locus of CG2 zebrafish assembly (haplotype 19D).
†Levels of pairwise percentage identity calculated with BLAST using predicted amino acid sequences.
‡Most closely matched genes identified from Zv9 zebrafish reference genome (haplotype 19B).
§Chromosome location.

trypsin-like peptide cleavage activity of PSMB10 remains similar to the constitutive PSMB7 subunit that it replaces on IFN stimulation. The sequences of this family of subunits (including zebrafish Psmb7 and Psmb13a as well as human PSMB7 and PSMB10), for the most part, maintain conserved negatively charged residue E53 or D53, which may provide complementarity within their trypsin-like active sites to the positively charged residues found at the C termini of their cleaved peptides. Thus, the E53Q substitution found in selected subunits, such as zebrafish Psmb13b, may alter the otherwise highly conserved trypsin-like activity of this family of proteasomal subunits.

Phylogenetic Analysis of Zebrafish TAP Subunits. The *abcb9* transporter gene (also called *TAP-like*) is common to all eukaryotes and considered the precursor of the heterodimeric *tap1* and *tap2* genes that arose during whole-genome duplications in ancestral vertebrates. Also found in jawless fish, such as lamprey (Fig. 5), the *abcb9* gene in jawed vertebrates may have more limited function in *MHCI* antigen processing (41, 42). The ancestral *abcb9* gene is largely monomorphic, unlike the polymorphic *tap1* and *tap2* genes found in many jawed vertebrates. For example, the derived *tap1* gene was found to be highly polymorphic in some species, such as *Xenopus* (43) and chicken (26). Similarly, polymorphic alleles for *tap2* have also been found in several species (Fig. 5), with divergent sequences ranging from >95% amino acid identity in chickens (26) to as low as 70% identity in *Xenopus*. In *Xenopus*, *tap2* lineages evolved transspecifically, shared across species that diverged on the order of 80–100 Mya (43).

Remarkably, phylogenetic analysis highlights the various zebrafish Tap2 subunits as the most divergent sequences among species with polymorphic Tap2 molecules (Fig. 5). Three major lineages are observed for the MHC-linked zebrafish Tap2 subunits: Tap2a/Tap2c, Tap2b/Tap2d, and Tap2e. The Tap2a subunit encoded by haplotypes A and B is relatively closely related with Tap2c, but Tap2c may actually represent a diverging tandem duplicate. Some relatively unusual substitutions, including T217V and R262D (*SI Appendix*, Table S3), may imply that Tap2c function is not conserved with that of the other zebrafish Tap2 subunits. Tap2c also has rather uncharacteristic insertions and deletions in its alignment relative to sequences from other *tap2* genes. For an additional zebrafish Tap2 lineage, the Tap2b and Tap2d subunits encoded by haplotypes A and D maintain 90% sequence identity, making them as divergent from one another as salmon Tap2a and Tap2b (91% sequence identity). The salmon *tap2b* gene is found in a duplicated MHCIB region (44) maintained 100 My after a salmonid-specific genome duplication event (45), providing a divergence time estimate consistent with these duplicated salmon *tap2* genes now being ∼90% identical.

Perhaps most striking from the tree (Fig. 5) is the deep divergence between the zebrafish Tap2d and Tap2e subunits (sharing only 50% amino acid sequence identity). This level of sequence divergence is comparable with the relationship shared between *Xenopus* and shark Tap2 subunits (51 to 59% identity) and also, the relationship shared between sequences for other diverse vertebrates (42 to 57% identity), species that have been independently evolving for ∼500 My (46). Sequences derived from polymorphic *tap2* alleles from chickens (26) each differ by ∼1–25 residues (>95% amino acid identity), similar to what has been found in rats (47). *Xenopus* species maintain divergent Tap2 sequences with over 200 amino acid substitutions (70% identity), representing lineages separated by 60–100 My of evolution (48). Therefore, the distinct zebrafish MHC haplotypes encode Tap2 molecules that are much more divergent than those found in other species previously described as maintaining highly polymorphic Tap2 molecules, such as rat, chicken, and *Xenopus*. These findings implicate independent evolution of *tap2* sequences among zebrafish core MHC haplotypes over exceptionally long periods of time, approaching the time to reach common ancestors among major vertebrate lineages.

Several residues have been shown to alter the transport specificity of peptide antigens (47) within Tap2 sequences (*SI Appendix*, Table S3). Positively charged R262 is associated with restricted peptide transport in rats with a restrictive allele 2B, and R262 is also encoded by the restrictive mouse *tap2* gene. In contrast, an uncharged residue Q262 is found in rats carrying a permissive peptide transport allele 2A, similar to the uncharged N262 encoded by the human permissive *tap2* gene. Both charged (R262) and uncharged (Q262) amino acids are found among

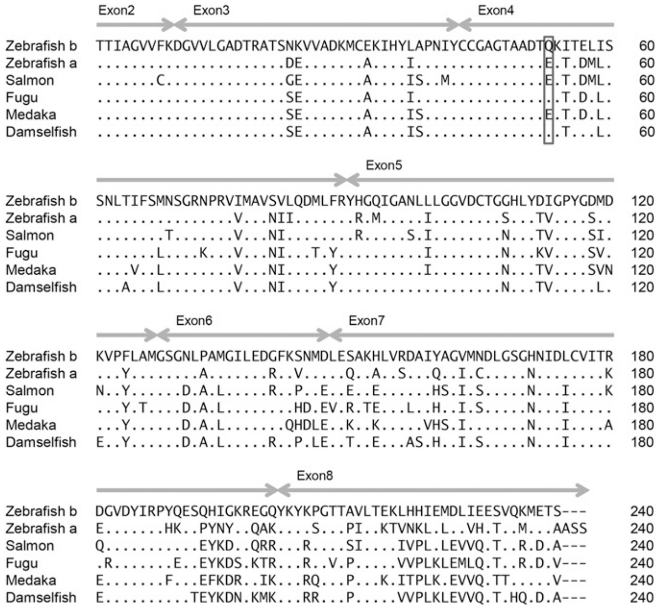

```
Zebrafish b  TTIAGVVFKDGVVLGADTRATSNKVVADKMCEKIHYLAPNIYCCGAGTAADTQKITELIS   60
Zebrafish a  ......................DE.......A...I................E.T.DML.   60
Salmon       .......C..............GE.......A...IS..M............E.T.DML.   60
Fugu         ......................SE.......A...I..................T.D.L.   60
Medaka       ......................SE.......A...IS...............E.T.D.L.   60
Damselfish   ......................SE.......A...IS.................T...L.   60

Zebrafish b  SNLTIFSMNSGRNPRVIMAVSVLQDMLFRYHGQIGANLLLGGVDCTGGHLYDIGPYGDMD  120
Zebrafish a  ................V...NII.......R.M.....I........S...TV....S..  120
Salmon       ........T.......V...NI........R.....S.I........N..TV....SI.  120
Fugu         .......L....K...V...NI...T.Y..........I........N..KV....SV.  120
Medaka       ....V..L........V...NI.....Y..........I........N..TV....SVN  120
Damselfish   ...A...L........V...NI.....Y...................N..TV.....L.  120

Zebrafish b  KVPFLAMGSGNLPAMGILEDGFKSNMDLESAKHLVRDAIYAGVMNDLGSGHNIDLCVITR  180
Zebrafish a  ...Y........A.......R..V.....Q..A..S...Q..I.C.....N........K  180
Salmon       N..Y......D.A.L.....R..P..E..E..E......HS.I.S.....N...I....K  180
Fugu         ...Y.T....D.A.L........HD.EV.R.TE...L..H..I.S.....N...I.....  180
Medaka       ...Y......D.A.L.......QHDLE..K..K.....VHS.I.......N...I....A  180
Damselfish   E..Y......D.A.L.....R..P.LE..T..E...AS.H..I.S.....N...I.....  180

Zebrafish b  DGVDYIRPYQESQHIGKREGQYKYKPGTTAVLTEKLHHIEMDLIEESVQKMETS---     240
Zebrafish a  E.......HK..PYNY..QAK....S...PI..KTVNKL.L..VH.T..M...AASS     240
Salmon       Q...........EYKD..QRR...R....SI....IVPL.LEVVQ.T..R.D.A---     240
Fugu         .R.......E..EYKDS.KTR...R..V.P.....VVPLKLEMLQ.T..R.D.V---     240
Medaka       E.......F...EFKDR..IK...RQ...P...K.ITPLK.EVVQ.TT.....V---     240
Damselfish   E..........TEYKDN.KMK...RR...P....VVPLKLEVVQ.T.HQ.D.A---     240
```

Fig. 4. Alignment of Psmb13 amino acid sequences. The deduced amino acid sequence for zebrafish Psmb13b (zebrafish b sequence from CG2 haplotype 19D) is highly divergent from zebrafish Psmb13a (zebrafish a sequence from Zv9 reference genome haplotype 19B). The first residue shown is the start of the mature protein after proteolytic cleavage exposes this essential catalytic residue (T1) of the active site (39). In 3D structures of proteasome subunits, position 53 (highlighted with a box) is located in close proximity to the catalytic site of the enzyme (40). The E53Q substitution is proposed to alter peptide cleavage specificity among divergent zebrafish Psmb13 molecules and also found in additional species. Identity to the sequence is shown with dots, and dashes indicate deletions. Double-headed arrows mark ranges of exons. Accession numbers are provided in *SI Appendix*, Table S8.

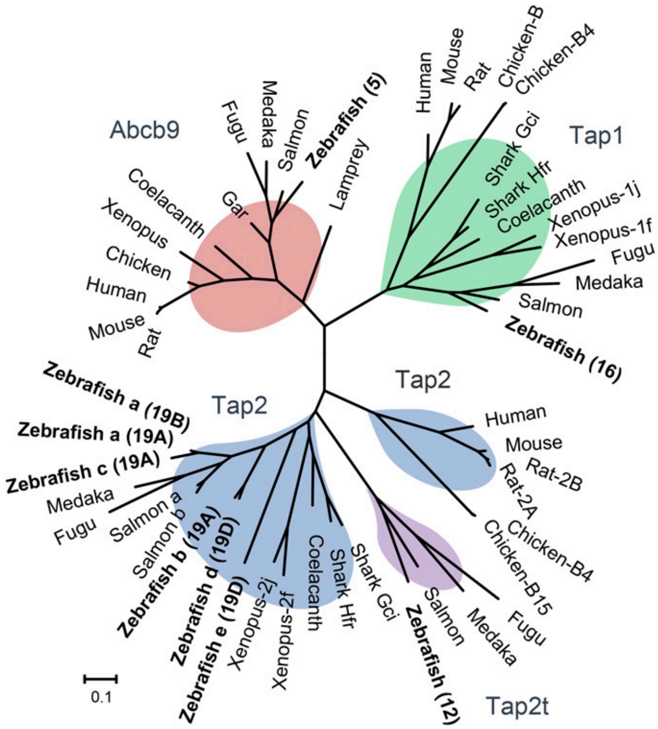

Fig. 5. Phylogenetic relationships for TAP subunits from zebrafish and additional vertebrates with divergent lineages. Deduced amino acid sequences were used to construct maximum likelihood trees. For the largely monomorphic non–MHC-linked Abcb9, Tap1, and Tap2t subunits, only the copies encoded by the Zv9 reference genome are shown. Bootstrap values are provided in *SI Appendix*, Fig. S8. Chromosome locations for zebrafish Tap2 subunits are provided in parentheses, including haplotype associations when applicable. Sequences are provided in Dataset S2.

sequences of five zebrafish Tap2 subunits. At a second functional site, a bulky F266 residue is found in mice and rats with restrictive alleles, whereas a less bulky hydrophobic residue L266 is found in humans and rats with permissive *tap2* genes. Both bulky (M266) and less bulky (L266) hydrophobic amino acids are also found in different zebrafish Tap2 subunits. At the start of the specificity loop is a third site, which has a T217A polymorphism that contributes to permissive peptide transport in rats. Both T217 and A217 residues are encoded among the divergent Tap2 subunits in zebrafish. These three polymorphisms are shared with functional polymorphisms found within Tap2 molecules from better characterized model organisms, providing evidence of potentially specialized functions for the divergent zebrafish Tap2 molecules. Our findings for proteasome subunit and Tap2 polymorphisms are in addition to other widespread polymorphisms found throughout the predicted peptide binding cleft of the linked *MHCI* genes (*SI Appendix*, Tables S9 and S10), which taken together, suggest strong likelihood for coevolution of peptide binding specificity throughout the entire zebrafish MHC pathway.

Proteasome and TAP Diversity Throughout Vertebrates. Comparative analysis of antigen processing genes throughout vertebrates yielded a number of surprises. Levels of divergence for alleles of zebrafish antigen processing and presentation genes exceeded levels found in other vertebrate species (Fig. 6). Higher levels of divergence were evident in the zebrafish *psmb9*, *psmb13*, *tap2*, and *MHCI* genes, particularly for *psmb13*.

We also uncovered divergent *psmb8f* as well as *psmb8a* lineages in coelacanths (Fig. 3). These ancient *psmb8* lineages cluster separately across sharks, teleosts, and coelacanths, implying that both lineages were present in the ancestors of all vertebrates, including tetrapods, such as humans and *Xenopus*. This observation supports the hypothesis that the somewhat less divergent *psmb8* lineages found in *Xenopus* were derived as the result of "erosion" of ancestral *psmb8f* sequences (49), representing fragmented transspecies polymorphism, and are not the result of convergent evolution as originally proposed.

In addition, sharks apparently have maintained a *psmb13* ortholog (Fig. 3), which is more closely related to the *psmb13* lineage from teleosts than to the *psmb10* lineage. However, unlike in teleosts, an additional gene representing the *psmb10* lineage may, instead, be absent from sharks. This shark *psmb13* gene appears to be largely monomorphic, unlike the salmon and zebrafish *psmb13* genes (Fig. 6). Lower sequence diversity would be consistent with a non–MHC-linked (*psmb10*-like) role for the *psmb13* gene in sharks.

Furthermore, paralleling previous findings in tetrapods (50), we determine that teleosts also have retained a non–MHC-linked *psmb10* gene (Fig. 3). Teleost *psmb10* is found outside of the core MHC, similar to human *PSMB10*, and these teleost *psmb10* genes maintain conserved synteny with human *psmb10* outside of their core MHC loci (*SI Appendix*, Fig. S3). Although previous studies had suggested that the teleost ortholog of human *PSMB10* was, instead, MHC-linked (17, 18), our findings clearly establish a non–MHC-linked gene as the true *PSMB10* ortholog in teleosts (Fig. 3). By also maintaining a largely monomorphic *psmb10* gene, teleosts may have additional capacity to support more specialized functions for their divergent *psmb13* genes.

Finally, we find that teleosts also have maintained a distinctive *tap2* gene, *tap2t*, which seems be teleost-specific (Fig. 5). This gene is in addition to their MHC-linked and highly divergent *tap2* lineages, indicating that the largely monomorphic non–MHC-linked gene, *tap2t* (*SI Appendix*, Fig. S4), may have additional conserved functions. In summary, teleosts maintain much higher diversity in their antigen processing genes than other vertebrates examined, including ancient sequence lineages across each of the MHC-linked antigen processing genes as well as conserved ancient paralogs *tap2t* (rather than only *tap2*), *psmb12* (rather than only *psmb9*), and *psmb13* (rather than only *psmb10*).

Discussion

In this study, we performed comparative genomic analysis of the core MHC region of zebrafish. Based on our de novo assembly of an alternative haplotype, we identified three antigen processing genes (*tap2d*, *psmb13b*, and *tap2e*) as well as additional MHC haplotype diversity. This diversity includes copy number differences for the *tap2*, *psmb12*, and *tapbp* genes and an inversion containing the three immunoproteasome genes. In addition to these genomic structural differences, ancient lineages are maintained for *psmb8*, *psmb9*, *psmb13*, and *tap2*. Taken together, these findings represent the most extensive diversity yet identified within the antigen processing genes of any species. Evidence of allelic variation for some antigen processing genes had been lacking (23), despite examination of numerous species across major vertebrate lineages. Therefore, our work addresses previously unrecognized gaps in our understanding of the evolution of vertebrate MHC regions, including identification of deeply divergent lineages for additional classes of proteasome and TAP subunits.

We have shown previously that zebrafish antigen presentation genes (*MHCI*) maintain copy number differences and divergent lineages among MHC haplotypes (31, 51). These findings for zebrafish antigen processing genes (including *tap2*, *psmb12*, and *psmb13*), thus, parallel and also greatly expand on the diversity that we previously described for the tightly linked *MHCI* genes. Unlike copy number differences in closely related genes found at many other loci, these antigen processing genes (*tap2*, *tapbp*, *psmb8*, *psmb9*, *psmb12*, and *psmb13*) and *MHCI* genes, although linked, are at most only weakly related to one another by sequence. Nevertheless, these genes remain functionally united by their various roles within a common antigen processing and presentation pathway.

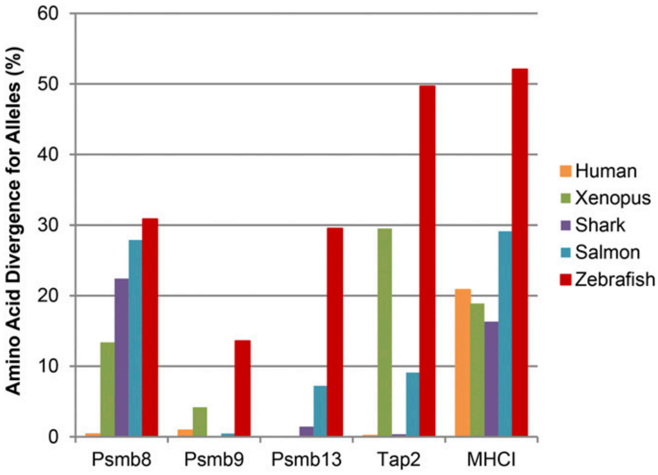

Fig. 6. Comparison of divergence levels for antigen processing and presentation genes. To compare the levels of divergence encoded by antigen processing and presentation genes from zebrafish and additional species, we searched for divergent alleles across vertebrates using the BLAST algorithm with expressed sequence tag (EST), transcriptome sequence assembly (TSA), and nonredundant (nr) GenBank databases. The most divergent alleles for each gene were identified and cataloged (accession numbers, divergence levels, and species identifiers are provided in *SI Appendix*, Table S11). Amino acid divergence (percentage) was calculated between these alleles using BLAST to identify those with the lowest amino acid identity, with divergence (%) = 100 (%) − identity (%). In many cases, these results are likely to underestimate diversity because of limitations, such as undersampling of sequences.

Five forms of proteasome assemblies have been described in mammals: constitutive proteasome, immunoproteasome, two forms of intermediate ("mixed") proteasome, and thymoproteasome (52). The number of different proteasome compositions seems limited by constraints of cooperative subunit assembly (53) (e.g., psmb8 before psmb9), because otherwise, at least twice this number of different assemblies might be expected. In zebrafish, a significantly larger number of distinct subunits (at least 12 variants vs. only 7 variants in mammals) offers potential for many additional proteasome assemblies. Even after accounting for cooperative assembly constraints, as many as 30 distinct combinations (25 unique to fish) could form in zebrafish that inherit two alternative MHC haplotypes (*SI Appendix*, Table S4). Moreover, based on predicted cleavage properties for the different subunits, different peptide repertoires are likely associated with these distinct zebrafish proteasome assemblies. Thus, even if most of these subunit combinations remain purely hypothetical, the additional proteasome subunits may nevertheless support a much greater diversity of peptide repertoires in zebrafish.

Widespread variation found among these different MHC pathway genes may be related to the specialization of antigen repertoires between haplotypes. This hypothesis is supported by several findings, including polymorphism that may lead to reduced trypsin-like activity for the Psmb13b subunit (Fig. 4). Furthermore, we identified additional polymorphism within the specificity loop of zebrafish Tap2 subunits (*SI Appendix*, Table S3), with substitutions identical to those shown in other species to control antigen transport specificity. These substitutions may be either permissive or restrictive to the transport of tryptic-like cleavage products having positively charged C termini. Polymorphisms associated with each of these linked zebrafish genes may help reinforce one another's functions by promoting compatible peptide antigen repertoires, as was previously observed for linked *tap2* and *MHCI* genes that coevolve distinctive peptide specificities in the rat and chicken (24, 26). Divergent sequences for the various zebrafish antigen processing genes may, therefore, be related to specialized functions, such as has been proposed for ancient transspecies polymorphism in *psmb8* also found in other species.

The *psmb8a* and *psmb8f* sequences from different zebrafish MHC haplotypes have been diverging for approximately 0.5 billion y (28). Here, we provide genomic context for *psmb8f*, which to date, has been studied primarily through amplicons and/or expressed transcripts. Our comparative genomic analysis shows that additional divergent sequences extend far beyond the boundaries of the zebrafish *psmb8f* gene, covering ∼100 kb of the MHC region. Surprisingly, distinct zebrafish MHC haplotypes maintain large regions of nearly unalignable sequence (*SI Appendix*, Fig. S2), comprising divergent gene lineages, copy number differences, and other structural changes. Despite this extensive sequence divergence, the *psmb8f* haplotype still retains representatives from all of the MHCI pathway genes (except *psmb12*), apparently leaving the integrity of this pathway intact.

We identified a chromosomal inversion (containing three divergent proteasome subunit genes for haplotype D) that may help further suppress recombination throughout this region. A similar mechanism by which chromosomal inversion suppresses recombination has been proposed for mouse MHC haplotypes (54). Because of stable haplotypes, coinherited genes may have accumulated their genetic diversity primarily because of this shared genomic location, maintaining deep lineages that parallel the divergent *psmb8f* and *mhc1uga* genes. Conversely, these genes may have developed their tight linkage primarily because of their cooperative and exclusive roles in enhancing shared MHC pathway function (23, 55). Maintaining a stable haplotypic structure would then help avoid sequence exchange events, such as recombination, that would interfere with coinherited gene function (56, 57) and thus, maintain efficiency of the MHC pathway.

Our results support a model where ancient whole-genome duplications produced a collection of precursor antigen processing and presentation genes in the ancestors of jawed vertebrates (Fig. 7*A*). After two rounds of whole-genome duplication, *psmb5* provided the precursors for *psmb8a*, *psmb8f*, and *psmb11*. Although *psmb5* was maintained as a constitutive proteasomal subunit, the three derived genes experienced reduced functional constraints as the paralogous *psmb8* genes gained IFN response and *psmb11* became thymus-specific. Similarly, constitutive *psmb6* duplicated to produce precursors for IFN-inducible *psmb9* as well as *psmb12*. In addition, *psmb7* served as the precursor for IFN-inducible *psmb10* and also, *psmb13*. These scenarios were mirrored by the *abcb9* gene, which yielded the heterodimeric *tap1* and *tap2*. Additionally, the Ig domain served as a foundation for formation of both *MHCI* and *MHCII* genes. A large proportion of these genes has maintained core MHC linkage throughout vertebrates, reflecting not only presumed primordial linkage important for evolution of the MHC pathway but also, continued linkage and coevolution optimizing MHC pathway function. An alternative model might consider *psmb12* and *psmb13* to be teleost-specific, similar to *tap2t* or *psmb11a*. However, evidence of shark sequences related to teleost *psmb13* suggests that these *psmb13* sequences are much older than teleosts. In addition, relative to the other proteasome genes (Fig. 3), the divergent nature of the *psmb12* and *psmb13* genes (surpassing even the divergent *psmb8* lineages that are shared across all major branches of vertebrates), instead, argues for a much more basal position for the *psmb12* and *psmb13* genes in ancestral vertebrates, most similar to the position of *psmb11*.

Accordingly, some of these genes, including *psmb13*, and allelic lineages, such as *psmb8f*, were subsequently lost in the mammalian branch of the tetrapod lineage. In certain vertebrate lineages, additional subsets of MHC pathway genes have been selectively lost, including *MHCII* genes in Atlantic cod (58) and nonconstitutive proteasome subunits in chickens (25). Nevertheless, immune systems within these species have apparently compensated for these genetic losses through other strategies, such as amplifying their *MHCI* gene number (58) or maintaining a larger number of *MHCI* and TAP alleles (26). Mammalian *MHCI* gene function may also have been shaped by the early loss of genes, such as *psmb13* and *psmb8f*. These losses combined with physical separation limiting the coevolution of their *MHCI*

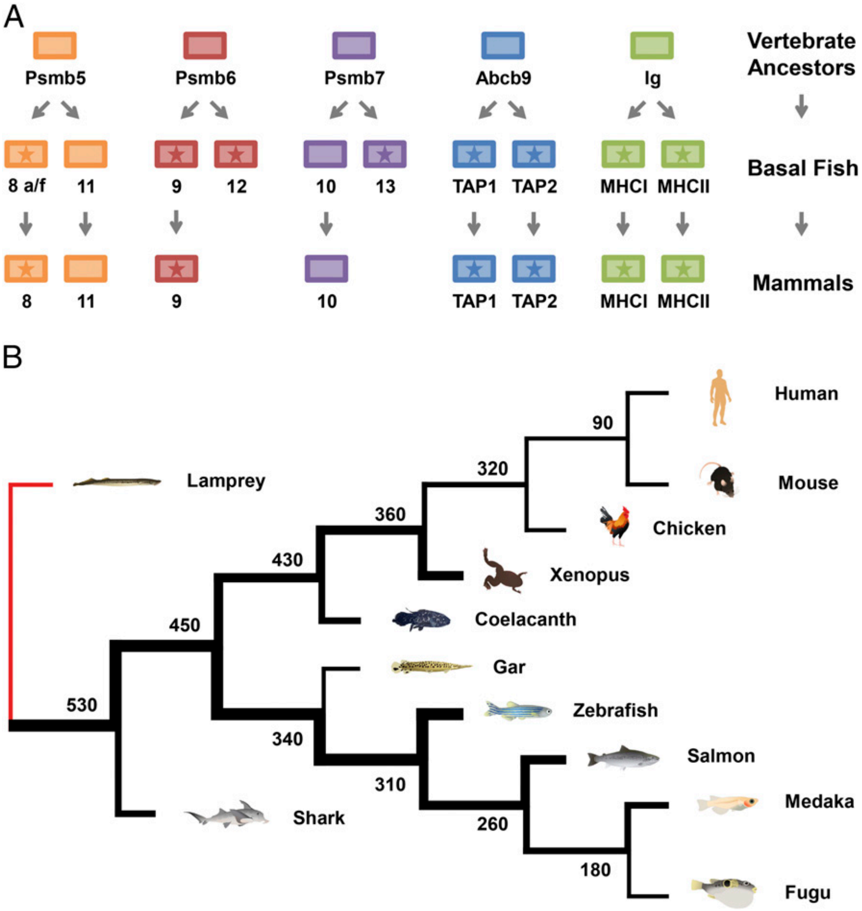

Fig. 7. Evolution of antigen processing and presentation genes throughout vertebrates. (*A*) The ancestors of jawed vertebrates underwent two rounds of whole-genome duplication. Many of the duplicated genes subsequently acquired roles in immune function, such as peptide binding/specificity, whereas early linkage within the proto-MHC likely facilitated coevolution of these genes to optimize MHC pathway function. Referred to here as basal fish, the last common ancestors of sharks, ray-finned fish, and lobe-finned fish maintained a higher number of MHC pathway genes than many extant vertebrates, particularly compared with mammals. This loss of mammalian MHC pathway diversity apparently included *psmb12* and *psmb13* as well as *psmb8f*. Genes with stars map to the core MHC region. Linkage differences are now found in some lineages, likely as a derived condition; for example, in teleost fish, the *MHCII* and *tap1* genes are no longer linked to the core MHC. (*B*) Lampreys as jawless fish completely lack an MHC pathway; however, sharks in the oldest surviving jawed vertebrate lineage had already evolved a complete MHC pathway similar to that of other jawed vertebrates. Ray-finned fish (e.g., zebrafish) as well as lobe-finned fish (e.g., coelacanths) lineages are shown to have maintained varying amounts of MHC pathway diversity, appearing more concentrated initially. Thicker lines represent greater sequence diversity for genes within the MHC pathway estimated by comparing available sequence lineages relative to other vertebrates examined. Sequence information is provided in *SI Appendix*, Tables S11–S13. Numbers at branch points indicate divergence time estimates in millions of years (38).

genes and antigen processing genes likely helped select for their hallmark collections of highly polymorphic classical *MHC* genes.

The exceptionally high levels of allelic divergence for genes, such as *psmb8* (Fig. 6), found across a full range of nonmammalian vertebrate species, including zebrafish, sharks, and coelacanths, exemplify the sharing of ancestral duplicated genes and ancient alleles for genes throughout the MHC pathway. Ancient sequence lineages for these genes have since been "eroded" to various extents across different vertebrate branches as well as occasionally lost in branches, such as mammals (Fig. 7*B*). The amount of remaining MHC pathway diversity may, thus, have had an important role in shaping vertebrate immunity.

Zebrafish are a relatively well-studied model organism, endowed with one of the highest quality "finished" vertebrate reference genomes (32). Zebrafish excel as a model to uncover gene function (59, 60) and are now advancing research in many fields, including stem cell biology (61, 62), cancer (63, 64), infectious disease (65, 66), and autoimmune disease studies (67, 68). In this context, we consider the identification of expressed genes in our zebrafish MHC assembly to be noteworthy. Based on earlier studies, genomic sequences were recognized as missing for *psmb8f* and *mhc1uga* (31) as well as for additional orphan genes such as *psmb9b* (32), a gene previously linked to an alternative MHC haplotype assembly (17). However, our examination of the genomic context for *psmb8f* also revealed three additional expressed genes: *psmb13b*, *tap2d*, and *tap2e*. These results indicate that sampling of immune genes may be far from saturated, even for well-studied model organisms, such as zebrafish.

Genes from divergent MHC pathways might be expected to strongly influence immune responses, particularly susceptibility to infectious disease, such as has been found in studies examining the impact of much more limited polymorphism (56, 69, 70). Zebrafish are now frequently used to model human disease; therefore, future studies could address the impact of these ancient immune sequences in settings such as viral infections. These studies may also inform our understanding of other populations such as humans, in whom these ancient genes have been lost, because this loss may have had important consequences for subsequent evolution of immune function.

Methods

Array-Based Capture and Whole-Exome Sequencing of Clonal Zebrafish. CG1 and CG2 represent two homozygous diploid (clonal) zebrafish lines (35, 36) derived by in-crossing isogenic offspring after two consecutive rounds of parthenogenesis (71). Each line was cloned from outbred AB zebrafish (72) carrying the golden allele (73). CG1 and CG2 are homozygous for distinct core MHC haplotypes C and D, respectively, among six divergent MHC haplotypes identified within laboratory AB stocks (31).

Genomic DNA samples from CG1 and CG2 (using four individuals from each line) were prepared for whole-exome analysis using previously described methods (59). Briefly, standard Illumina primers were used to amplify libraries and barcode different DNA samples, which were pooled before target enrichment. Agilent SureSelect Target Enrichment relied on 120-bp baits designed against all annotated protein coding genes from the Ensembl Zv9 release of the zebrafish genome. Captured DNA was then sequenced on an Illumina HiSeq2000 instrument using a single lane. Reads were aligned with the Burrows–Wheeler Aligner against the Zv9 reference genome.

SNPs were called by using a combination of GATK Unified Genotyper, SAMtools mpileup, and QCALL. SNPs were identified as either heterozygous or homozygous after passing filters from all three SNP callers with additional quality controls as described (59). Approximately 400,000–500,000 SNPs were identified for each clonal line (*SI Appendix*, Table S5). However, within each of two clonal lines, the vast majority (>98.2%) of SNPs were called as homozygous, consistent with double-haploid derivation of isogenic zebrafish (71).

Whole-Genome Sequencing and de Novo Assembly. Genomic DNA from a CG2 clonal zebrafish was sequenced using an Illumina HiSeq2500 instrument, producing over 38 Gb 2 × 100 paired end read data with ∼25× sequence coverage. Illumina adapters were removed using SeqPrep (74) version 1.1, and reads were filtered for quality with Trimmomatic (75) version 0.3. After filtering and clipping, read quality was assessed using FastQC (76). De novo assembly was generated using the SOAPdenovo2 (77) algorithm with optimized parameters (kmer value of 59). The resulting de novo assembly had an N50 (median scaffold size of genomic assembly) value of 34 kb, with 5.7% Ns (unknown bases) and scaffolds covering ∼82% of the genome. Scaffolds larger than 1 kb were aligned against the zebrafish Zv9 reference genome assembly using the nucmer tool from MUMmer (78) version 3.23. We used Augustus (79) to generate gene models from our genomic scaffolds as well as Webscipio (80) to help improve gene annotation. Within the core MHC locus, conserved flanking genes, including *daxx* and *tapbp*, anchor CG2 genomic scaffold 13,206, which also includes the 5′ portion of *mhc1uga*. The 3′ portion of *mhc1uga* is included within scaffold 51,738. Similarly, *brd2a* and *hsd17b8* within the core MHC locus anchor scaffold 2,546, which also includes *tap2e* and *psmb8f* as well as the 3′ portion of *psmb13b*. The 5′ portion of *psmb13b* is found within scaffold 15,837, which also includes the *psmb9* and *tap2d* genes.

RNA-Seq Transcriptome Assembly and Sequence Analysis. Generation of the CG2 RNA-Seq library was described previously (51). Briefly, kidney, spleen, intestine, and gill were dissected and pooled to purify RNA from immune tissues of CG2 clonal zebrafish. Paired end 2 × 100-bp reads were generated with an Illumina HiSeq2000 instrument and assembled using Trinity (81). Amino acid sequences were aligned using MUSCLE (82). Phylogenetic trees were constructed using the maximum likelihood method within the MEGA6 program (83) and bootstrapped with 500 replicates. Pairwise amino acid identity was calculated using BLAST (84). Exome data were visualized using the IGV Viewer (85). Transcripts associated with zebrafish core MHC haplotype D are provided in Dataset S3, predicted amino acid sequences for the CG2 haplotype D antigen processing gene transcripts are provided in Dataset S4, and genomic scaffold sequences identified from haplotype D are provided in Dataset S5.

Nomenclature for Proteasome Subunits. Nomenclature for proteasome and TAP genes has remained inconsistent across species and studies, particularly for genes not found in the mammalian lineage. Here, we provide systematic nomenclature that encompasses identified as well as additional proteasome genes (*SI Appendix*, Table S6). This nomenclature takes into account phylogenomic analysis, including conserved syntenies, and is based on original gene nomenclature proposals. All zebrafish gene names have been approved by the zebrafish nomenclature committee.

An MHC-linked zebrafish gene in the *psmb6/9* family, first described as *psmb11* (29), has also been called *psmb9l* (18). However, the name *psmb11* is currently problematic, because it conflicts with nomenclature for distinct vertebrate genes also called *psmb11* (37) (e.g., zebrafish *psmb11a* and *psmb11b* that are found outside the core MHC). These two latter zebrafish genes belong to the conserved *psmb5/8/11* family (Fig. 3), where subunits follow the (*psmb* X, X + 3, and X + 6) numbering schema across vertebrates. *Psmb9l* is another name used for the former MHC-linked gene, but this "*psmb9*-like" gene is actually highly divergent from the *psmb9* lineage, contributing a distinctive third lineage branch across teleosts (Fig. 3). Furthermore, the appended letter for *psmb9l* may become confusing when in use with genes with other appended letters, such as *psmb9a*. These considerations led us to propose the name *psmb12* (*SI Appendix*, Table S6), recognizing the *psmb6/9/12* gene family. Our proposed name reflects the status of *psmb12* as the most divergent branch within this family and provides parallel (*psmb* Y, Y + 3, and Y + 6) nomenclature while using the next gene name available.

Another proteasome subunit gene discovered in the teleost core MHC was originally described as *psmb12* (29), recognizing that, although clearly related, it is also quite distinct from tetrapod *psmb10*. Subsequently, this gene was annotated as *psmb10* in fugu (18) and more recently, other fish species. However, the *psmb10* assignment for this gene is justified only if another conserved, non–MHC-linked *psmb10* ortholog is truly absent from bony fish genomes. Surprisingly, we found evidence of a conserved non–MHC-linked *psmb10* gene throughout bony fish species (Fig. 3). This finding implies that *psmb10* was already found outside of the MHC in the common ancestors of tetrapods and bony fish, which is inconsistent with a more derivative tetrapod *psmb10* translocation event suggested in previous models. Thus, our nomenclature assigns *psmb10* as an immunoproteasome subunit within most vertebrate species, including bony fish, where it is unlinked to the MHC.

We propose that the MHC-linked zebrafish gene formerly known as *psmb12* or *psmb10* be renamed *psmb13* (*SI Appendix*, Table S6). The *psmb13* gene is conserved across teleosts and to a lesser degree, sharks (Fig. 3), suggesting ancient conserved function for this gene that may curiously now be missing from other vertebrates, such as humans. Our proposal, thus, assigns *psmb13* as the third divergent lineage belonging to the *psmb7/10/13* gene family following parallel nomenclature structure (*psmb* Z, Z + 3, and Z + 6). In summary, the *psmb7/10/13* gene family forms the third and final lineage trifurcation among the *psmb5–13* genes (Fig. 3).

Nomenclature for TAP Subunits. We also propose names for seven zebrafish TAP genes (*SI Appendix*, Table S7) based on the original nomenclature (17), including *tap2a* and *tap2b* (rather than *abcb3l1* and *abcb3*, respectively). *Tap2*, *tap1*, and ancestral *abcb9* form an ancient lineage trifurcation across jawed vertebrates (Fig. 5). We propose that zebrafish *abcb2* be renamed *tap1* (*SI Appendix*, Table S7) to maintain consistency with nomenclature used for orthologous genes, such as in humans (86).

Furthermore, within the larger *tap2* branch, several genes cluster together as distinct from the *tap2* genes found in the MHC region of their respective teleost species (Fig. 5). Our proposed name for the identified zebrafish gene is *tap2t*, reflecting recognition of this gene as a teleost-specific member of the larger *tap2* family (Fig. 5). *Tap2t* is not linked to the core MHC region but has conserved synteny among teleosts (*SI Appendix*, Fig. S4). Similar to the other Tap2 subunits in zebrafish, Tap2t conserves key residues within a specificity loop predicted to interact with peptides (*SI Appendix*, Table S3). In summary, this zebrafish proteasome and TAP gene nomenclature remains consistent with that in humans as well as additional vertebrates (44). We believe that this proposal will help further promote nomenclature consistency across species, facilitating future comparative studies.

ACKNOWLEDGMENTS. We thank Ian Sealy for help with exome data, Betsy Scholl for bioinformatics support, Sergei Revskoy for clonal zebrafish, and Daniel Ocampo Daza for vertebrate illustrations. We thank Wilfredo Marin and Haley Engel at the University of Chicago for excellent care of our zebrafish colony. We also thank Pieter Faber from the University of Chicago Genomics core and Cancer Center Support Grant (P30 CA014599) for sequencing support. This work was funded, in part, by a Chicago Biomedical Consortium Postdoctoral Research Grant with support from the Searle Funds at the Chicago Community Trust and, also, the University of Chicago Cancer Research Foundation Auxiliary Board. D.J.W. was supported by the National Evolutionary Synthesis Center (National Science Foundation Grant EF-0905606).

1. Shiina T, Hosomichi K, Inoko H, Kulski JK (2009) The HLA genomic loci map: Expression, interaction, diversity and disease. *J Hum Genet* 54(1):15–39.
2. Klein J, Sato A, Nagl S, O'hUigín C (1998) Molecular trans-species polymorphism. *Annu Rev Ecol Syst* 29:1–21.
3. Piontkivska H, Nei M (2003) Birth-and-death evolution in primate MHC class I genes: Divergence time estimates. *Mol Biol Evol* 20(4):601–609.
4. Raymond CK, et al. (2005) Ancient haplotypes of the HLA Class II region. *Genome Res* 15(9):1250–1257.
5. Klein J, Sato A, Nikolaidis N (2007) MHC, TSP, and the origin of species: From immunogenetics to evolutionary genetics. *Annu Rev Genet* 41:281–304.
6. Barreiro LB, Quintana-Murci L (2010) From evolutionary genetics to human immunology: How selection shapes host defence genes. *Nat Rev Genet* 11(1):17–30.
7. Okamura K, Ototake M, Nakanishi T, Kurosawa Y, Hashimoto K (1997) The most primitive vertebrates with jaws possess highly polymorphic MHC class I genes comparable to those of humans. *Immunity* 7(6):777–790.
8. Flajnik MF, et al. (1999) Two ancient allelic lineages at the single classical class I locus in the Xenopus MHC. *J Immunol* 163(7):3826–3833.
9. Shum BP, et al. (2001) Modes of salmonid MHC class I and II evolution differ from the primate paradigm. *J Immunol* 166(5):3297–3308.
10. Aoyagi K, et al. (2002) Classical MHC class I genes composed of highly divergent sequence lineages share a single locus in rainbow trout (Oncorhynchus mykiss). *J Immunol* 168(1):260–273.
11. Jaratlerdsiri W, et al. (2014) Comparative genome analyses reveal distinct structure in the saltwater crocodile MHC. *PLoS One* 9(12):e114631.
12. Venkatesh B, et al. (2014) Elephant shark genome provides unique insights into gnathostome evolution. *Nature* 505(7482):174–179.
13. Grimholt U, et al. (2015) A comprehensive analysis of teleost MHC class I sequences. *BMC Evol Biol* 15(1):32.
14. Ng JHJ, et al. (2016) Evolution and comparative analysis of the bat MHC-I region. *Sci Rep* 6:21256.
15. Ohta Y, McKinney EC, Criscitiello MF, Flajnik MF (2002) Proteasome, transporter associated with antigen processing, and class I genes in the nurse shark Ginglymostoma cirratum: Evidence for a stable class I region and MHC haplotype lineages. *J Immunol* 168(2):771–781.
16. Flajnik MF, Ohta Y, Namikawa-Yamada C, Nonaka M (1999) Insight into the primordial MHC from studies in ectothermic vertebrates. *Immunol Rev* 167(1):59–67.
17. Michalová V, Murray BW, Sültmann H, Klein J (2000) A contig map of the Mhc class I genomic region in the zebrafish reveals ancient synteny. *J Immunol* 164(10):5296–5305.

18. Clark MS, Shaw L, Kelly A, Snell P, Elgar G (2001) Characterization of the MHC class I region of the Japanese pufferfish (Fugu rubripes). *Immunogenetics* 52(3-4):174–185.
19. Matsuo MY, Asakawa S, Shimizu N, Kimura H, Nonaka M (2002) Nucleotide sequence of the MHC class I genomic region of a teleost, the medaka (Oryzias latipes). *Immunogenetics* 53(10-11):930–940.
20. Ohta Y, Goetz W, Hossain MZ, Nonaka M, Flajnik MF (2006) Ancestral organization of the MHC revealed in the amphibian Xenopus. *J Immunol* 176(6):3674–3685.
21. Kaufman J (2013) Antigen processing and presentation: Evolution from a bird's eye view. *Mol Immunol* 55(2):159–161.
22. Siddle HV, et al. (2009) MHC-linked and un-linked class I genes in the wallaby. *BMC Genomics* 10(1):310.
23. Ohta Y, Flajnik MF (2015) Coevolution of MHC genes (LMP/TAP/class Ia, NKT-class Ib, NKp30-B7H6): lessons from cold-blooded vertebrates. *Immunol Rev* 267(1):6–15.
24. Joly E, et al. (1998) Co-evolution of rat TAP transporters and MHC class I RT1-A molecules. *Curr Biol* 8(3):169–172.
25. Erath S, Groettrup M (2015) No evidence for immunoproteasomes in chicken lymphoid organs and activated lymphocytes. *Immunogenetics* 67(1):51–60.
26. Walker BA, et al. (2011) The dominantly expressed class I molecule of the chicken MHC is explained by coevolution with the polymorphic peptide transporter (TAP) genes. *Proc Natl Acad Sci USA* 108(20):8396–8401.
27. Bingulac-Popovic J, et al. (1997) Mapping of mhc class I and class II regions to different linkage groups in the zebrafish, Danio rerio. *Immunogenetics* 46(2):129–134.
28. Tsukamoto K, Miura F, Fujito NT, Yoshizaki G, Nonaka M (2012) Long-lived dichotomous lineages of the proteasome subunit beta type 8 (PSMB8) gene surviving more than 500 million years as alleles or paralogs. *Mol Biol Evol* 29(10):3071–3079.
29. Murray BW, Sültmann H, Klein J (1999) Analysis of a 26-kb region linked to the Mhc in zebrafish: Genomic organization of the proteasome component β/transporter associated with antigen processing-2 gene cluster and identification of five new proteasome β subunit genes. *J Immunol* 163(5):2657–2666.
30. Tsukamoto K, et al. (2009) Dichotomous haplotypic lineages of the immunoproteasome subunit genes, PSMB8 and PSMB10, in the MHC class I region of a Teleost Medaka, Oryzias latipes. *Mol Biol Evol* 26(4):769–781.
31. McConnell SC, Restaino AC, de Jong JLO (2014) Multiple divergent haplotypes express completely distinct sets of class I MHC genes in zebrafish. *Immunogenetics* 66(3): 199–213.
32. Howe K, et al. (2013) The zebrafish reference genome sequence and its relationship to the human genome. *Nature* 496(7446):498–503.
33. Flajnik MF, Kasahara M (2001) Comparative genomics of the MHC: Glimpses into the evolution of the adaptive immune system. *Immunity* 15(3):351–362.
34. Flajnik MF, Kasahara M (2010) Origin and evolution of the adaptive immune system: Genetic events and selective pressures. *Nat Rev Genet* 11(1):47–59.
35. Smith AC, et al. (2010) High-throughput cell transplantation establishes that tumor-initiating cells are abundant in zebrafish T-cell acute lymphoblastic leukemia. *Blood* 115(16):3296–3303.
36. Mizgirev IV, Revskoy S (2010) A new zebrafish model for experimental leukemia therapy. *Cancer Biol Ther* 9(11):895–902.
37. Sutoh Y, et al. (2012) Comparative genomic analysis of the proteasome β5t subunit gene: Implications for the origin and evolution of thymoproteasomes. *Immunogenetics* 64(1):49–58.
38. Hedges S, Kumar S (2009) *The Timetree of Life* (Oxford Univ Press, New York).
39. Ferrington DA, Gregerson DS (2012) Immunoproteasomes: Structure, function, and antigen presentation. *Prog Mol Biol Transl Sci* 109:75–112.
40. Huber EM, et al. (2012) Immuno- and constitutive proteasome crystal structures reveal differences in substrate and inhibitor specificity. *Cell* 148(4):727–738.
41. Uinuk-ool TS, et al. (2003) Identification and characterization of a TAP-family gene in the lamprey. *Immunogenetics* 55(1):38–48.
42. Herget M, Tampé R (2007) Intracellular peptide transporters in human—compartmentalization of the "peptidome." *Pflugers Arch* 453(5):591–600.
43. Ohta Y, et al. (2003) Two highly divergent ancient allelic lineages of the transporter associated with antigen processing (TAP) gene in Xenopus: Further evidence for co-evolution among MHC class I region genes. *Eur J Immunol* 33(11):3017–3027.
44. Lukacs MF, et al. (2007) Genomic organization of duplicated major histocompatibility complex class I regions in Atlantic salmon (Salmo salar). *BMC Genomics* 8(1):251–266.
45. Berthelot C, et al. (2014) The rainbow trout genome provides novel insights into evolution after whole-genome duplication in vertebrates. *Nat Commun* 5(3657):3657.
46. Blair JE, Hedges SB (2005) Molecular phylogeny and divergence times of deuterostome animals. *Mol Biol Evol* 22(11):2275–2284.
47. Deverson EV, et al. (1998) Functional analysis by site-directed mutagenesis of the complex polymorphism in rat transporter associated with antigen processing. *J Immunol* 160(6):2767–2779.
48. Ohta Y, et al. (1999) Identification and genetic mapping of Xenopus TAP2 genes. *Immunogenetics* 49(3):171–182.
49. Huang C-H, Tanaka Y, Fujito NT, Nonaka M (2013) Dimorphisms of the proteasome subunit beta type 8 gene (PSMB8) of ectothermic tetrapods originated in multiple independent evolutionary events. *Immunogenetics* 65(11):811–821.
50. Kasahara M, et al. (1996) Chromosomal localization of the proteasome Z subunit gene reveals an ancient chromosomal duplication involving the major histocompatibility complex. *Proc Natl Acad Sci USA* 93(17):9096–9101.
51. Dirscherl H, Yoder JA (2015) A nonclassical MHC class I U lineage locus in zebrafish with a null haplotypic variant. *Immunogenetics* 67(9):501–513.
52. McCarthy MK, Weinberg JB (2015) The immunoproteasome and viral infection: A complex regulator of inflammation. *Front Microbiol* 6:21.
53. Guillaume B, et al. (2010) Two abundant proteasome subtypes that uniquely process some antigens presented by HLA class I molecules. *Proc Natl Acad Sci USA* 107(43): 18599–18604.
54. Hammer MF, Schimenti J, Silver LM (1989) Evolution of mouse chromosome 17 and the origin of inversions associated with t haplotypes. *Proc Natl Acad Sci USA* 86(9): 3261–3265.
55. Kaufman J (2015) Co-evolution with chicken class I genes. *Immunol Rev* 267(1):56–71.
56. Kaufman J (2015) What chickens would tell you about the evolution of antigen processing and presentation. *Curr Opin Immunol* 34:35–42.
57. Tuncel J, et al.; EURATRANS Consortium (2014) Natural polymorphisms in Tap2 influence negative selection and CD4:CD8 lineage commitment in the rat. *PLoS Genet* 10(2):e1004151.
58. Star B, et al. (2011) The genome sequence of Atlantic cod reveals a unique immune system. *Nature* 477(7363):207–210.
59. Kettleborough RNW, et al. (2013) A systematic genome-wide analysis of zebrafish protein-coding gene function. *Nature* 496(7446):494–497.
60. Phillips JB, Westerfield M (2014) Zebrafish models in translational research: Tipping the scales toward advancements in human health. *Dis Model Mech* 7(7):739–743.
61. Barbosa JS, et al. (2015) Neurodevelopment. Live imaging of adult neural stem cell behavior in the intact and injured zebrafish brain. *Science* 348(6236):789–793.
62. Tamplin OJ, et al. (2015) Hematopoietic stem cell arrival triggers dynamic remodeling of the perivascular niche. *Cell* 160(1-2):241–252.
63. White R, Rose K, Zon L (2013) Zebrafish cancer: The state of the art and the path forward. *Nat Rev Cancer* 13(9):624–636.
64. Yen J, White RM, Stemple DL (2014) Zebrafish models of cancer: Progress and future challenges. *Curr Opin Genet Dev* 24:38–45.
65. Goody MF, Sullivan C, Kim CH (2014) Studying the immune response to human viral infections using zebrafish. *Dev Comp Immunol* 46(1):84–95.
66. Cronan MR, Tobin DM (2014) Fit for consumption: Zebrafish as a model for tuberculosis. *Dis Model Mech* 7(7):777–784.
67. Quintana FJ, et al. (2010) Adaptive autoimmunity and Foxp3-based immunoregulation in zebrafish. *PLoS One* 5(3):e9478.
68. Cusick MF, Libbey JE, Trede NS, Eckels DD, Fujinami RS (2012) Human T cell expansion and experimental autoimmune encephalomyelitis inhibited by Lenaldekar, a small molecule discovered in a zebrafish screen. *J Neuroimmunol* 244(1-2):35–44.
69. Grimholt U, et al. (2003) MHC polymorphism and disease resistance in Atlantic salmon (Salmo salar); facing pathogens with single expressed major histocompatibility class I and class II loci. *Immunogenetics* 55(4):210–219.
70. International HIV Controllers Study, et al. (2010) The major genetic determinants of HIV-1 control affect HLA Class I peptide presentation. *Science* 330(6010):1551–1557.
71. Mizgirev I, Revskoy S (2010) Generation of clonal zebrafish lines and transplantable hepatic tumors. *Nat Protoc* 5(3):383–394.
72. ZFIN The Zebrafish Model Organism Database (2016) *Wild-Type Line AB*. Available at https://zfin.org/ZDB-GENO-960809-7. Accessed April 5, 2016.
73. Lamason RL, et al. (2005) SLC24A5, a putative cation exchanger, affects pigmentation in zebrafish and humans. *Science* 310(5755):1782–1786.
74. St. John J (2013) *SeqPrep*. Available at https://github.com/jstjohn/SeqPrep. Accessed September 11, 2014.
75. Bolger AM, Lohse M, Usadel B (2014) Trimmomatic: A flexible trimmer for Illumina sequence data. *Bioinformatics* 30(15):2114–2120.
76. Andrews S (2012) FastQC. Available at: www.bioinformatics.babraham.ac.uk/projects/fastqc/. Accessed September 11, 2014.
77. Luo R, et al. (2012) SOAPdenovo2: An empirically improved memory-efficient short-read de novo assembler. *Gigascience* 1(1):18.
78. Kurtz S, et al. (2004) Versatile and open software for comparing large genomes. *Genome Biol* 5(2):R12.
79. Stanke M, Diekhans M, Baertsch R, Haussler D (2008) Using native and syntenically mapped cDNA alignments to improve de novo gene finding. *Bioinformatics* 24(5): 637–644.
80. Hatje K, et al. (2011) Cross-species protein sequence and gene structure prediction with fine-tuned Webscipio 2.0 and Scipio. *BMC Res Notes* 4(1):265.
81. Grabherr MG, et al. (2011) Full-length transcriptome assembly from RNA-Seq data without a reference genome. *Nat Biotechnol* 29(7):644–652.
82. Edgar RC (2004) MUSCLE: Multiple sequence alignment with high accuracy and high throughput. *Nucleic Acids Res* 32(5):1792–1797.
83. Tamura K, Stecher G, Peterson D, Filipski A, Kumar S (2013) MEGA6: Molecular evolutionary genetics analysis version 6.0. *Mol Biol Evol* 30(12):2725–2729.
84. Altschul SF, et al. (1997) Gapped BLAST and PSI-BLAST: A new generation of protein database search programs. *Nucleic Acids Res* 25(17):3389–3402.
85. Robinson JT, et al. (2011) Integrative genomics viewer. *Nat Biotechnol* 29(1):24–26.
86. Gray KA, Yates B, Seal RL, Wright MW, Bruford EA (2015) Genenames.org: The HGNC resources in 2015. *Nucleic Acids Res* 43(Database issue):D1079–D1085.
87. Kandil E, et al. (1996) Isolation of low molecular mass polypeptide complementary DNA clones from primitive vertebrates. Implications for the origin of MHC class I-restricted antigen presentation. *J Immunol* 156(11):4245–4253.